Spin Density Matrix Elements for Exclusive ρ^0 Meson Muoproduction at COMPASS

W. Augustyniak
on behalf of the COMPASS Collaboration

National Centre for Nuclear Research Warsaw
w.augustyniak@nbcj.gov.pl

July 20, 2021

*Proceedings for the XXVIII International Workshop
on Deep-Inelastic Scattering and Related Subjects,
Stony Brook University, New York, USA, 12-16 April 2021*

Abstract

Spin density matrix elements were extracted from COMPASS data for exclusive ρ^0 meson muoproduction on a liquid hydrogen target. The measurement cover the kinematic range of 1.0 $(\text{GeV}/c)^2 < Q^2 < 10.0 \ (\text{GeV}/c)^2$, 5.0 $\text{GeV}/c^2 < W < 17.0 \ \text{GeV}/c^2$ and 0.01 $(\text{GeV}/c)^2 < p_T^2 < 0.5 \ (\text{GeV}/c)^2$. Here, W denotes the mass of the final hadronic system, Q^2 the virtuality of the exchanged photon and p_T the transverse momentum of the ρ^0 meson with respect to the virtual-photon direction. We observe a violation of s-channel helicity conservation for the transition $\gamma_T^* \rightarrow \rho_L^0$. Additionally, we find a dominant contribution of the natural-parity-exchange transitions.

1   Introduction

Exclusive ρ^0 muoproduction is studied using the process $\mu + p \rightarrow \mu' + p' + \rho^0$, which in the one-photon-exchange approximation is described by the interaction of a virtual photon with the target proton $\gamma^* + p \rightarrow p' + \rho^0$. Spin Density Matrix Elements (SDME) describe

transitions between specified spin states of the virtual photon, the target proton, the produced vector meson and the recoil proton and depend on kinematic variables Q^2, p_T^2 and W. They serve to establish the hierarchy of amplitudes, to probe dominant amplitudes with s-channel helicity conservation (SCHC), and to study Natural-Parity-Exchange (NPE), Unatural-Parity-Exchange (UPE) as well as spin-flip transitions. The processes with high virtuality of Q^2 of the virtual photon and low values of squared four momentum transfer t, known as Hard Exclusive Meson Production (HEMP), are a useful tool to access General Parton Distributions (GPDs). The HEMP amplitude factorises into a hard-scattering part, which is calculable in perturbative QCD (pQCD), and soft part [1]. The soft part contains GPDs that describing structure of nucleon. The model by Goloskokov and Kroll (GK model) from Refs. [2]-[6] describes for both longitudinally and transversely polarised virtual photons the cross sections, SDMEs as well as target and beam-spin asymmetries for vector- and pseudoscalar-meson leptoproduction. The GK model includes chiral-even and chiral-odd GPDs. It predicts contributions by chiral-odd GPDs in pseudoscalar meson production, and spin-flips and UPE processes in vector-mesons production.
The SDMEs are presented in the Schilling and Wolf representations [7].

2 Experiment and data processing

The analysis is based on the data taken by COMPASS in 2012. The experiment used the 160 GeV μ^+ (μ^-) beams with -80% (+80%) longitudinal polarisation and a liquid hydrogen target. The exclusive process with ρ^0 meson production was selected:

$\mu p \rightarrow \mu' p' \rho^0$, $\rho^0 \rightarrow \pi^+ \pi^-$ (BR=100%).

The accepted events in the analysis contain the scattered muon track and two hadron tracks with opposite charges. Additional requirements were imposed on the invariant mass of the two pions and missing energy. The invariant mass of the two pions $M_{\pi\pi}$ is presented in Fig. 1 by the
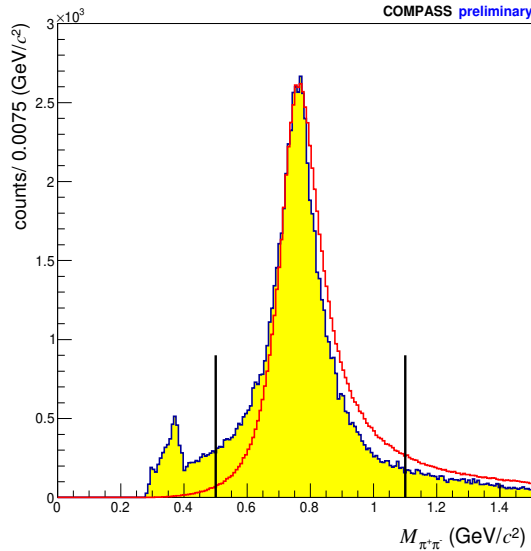
Figure 1: Distribution of the π^+ π^- invariant mass for experimental data (blue) and for HEPGEN (red). The invariant mass from HEPGEN distribution is normalised to the data in the region 0.75 GeV/c^2 < $M_{\pi\pi}$ < 0.77 GeV/c^2, where the vertical lines indicate the applied limits.

blue histogram. The vertical lines indicate the limits of the analysed region (0.5 GeV/c^2 < $M_{\pi\pi}$ < 1.1 GeV/c^2). Background coming from exclusive production of ϕ and its decay $\phi \to K^+K^-$, where the kaons are misidentified as pions is expected and seen at $M_{\pi\pi}$ < 0.4 GeV/c^2. After applying the indicated selection on the invariant mass this background is removed.

The experimental data are compared to the events generated by HEPGEN [8]. The observed skewing of the invariant mass distribution for data with respect to MC is due to the small contribution of nonresonant pion-pairs and its interference with resonant production [9] .

The exclusivity of ρ^0 events was ensured by $E_{miss} = \frac{M_x^2 - M_p^2}{2M_p}$, with the missing mass squared $M_x^2 = (p + q - p_{\pi^+} - p_{\pi^-})^2$, where p, q, p_{π^+} and p_{π^-}, are the four-momenta of the proton, photon, and two pions , respectively.

In Fig. 2, the missing-energy distribution is shown as red points, while the blue points cor-
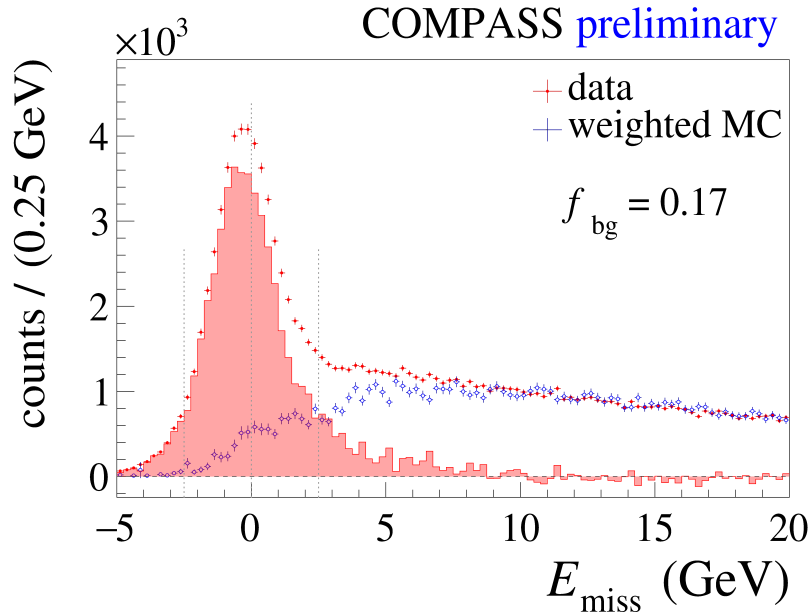
Figure 2: The missing-energy distribution from experimental data (red point) compared to the distribution of SIDIS events from LEPTO MC (blue points). The MC distribution is normalised to the data of region 7 GeV < E_{miss} < 20 GeV. The background-corrected distribution for data is shown as shaded histogram. The vertical indicate the limits of exclusive region. Each LEPTO MC event is reweighted by an E_{miss} dependent weight that is calculated using the both experimental and simulated data with the same-charge hadron pairs.

respond to background evaluated by MC LEPTO generator [10]. The amount of background f_{bg} in the signal window $|E_{miss}|$ < 2.5 GeV was estimated to be 17% for the entire analysed region. The ratio of the of the non-exclusive events in the signal window depends on Q^2, p_T^2 and W. The selected sample consists of 23785 events for μ^+ and 28472 for μ^-.

The SDMEs were determined by using an unbinned maximum likelihood method by fitting the function $\mathcal{W}(\Phi, \phi, \cos\Theta)$ (for definitions of $\mathcal{W}$ distribution and angles Φ, ϕ, $\cos\Theta$ see Ref. [11]) to the experimental three-dimensional angular distribution of ρ^0 production and decay. The fitted distribution is a weighted superposition of $\mathcal{W}$ distributions for exclusive events and non-exclusive background. The parameters describing the background angular distributions were pre-determined by fitting either angular distributions of events in the signal window from LEPTO MC or distributions for the real data in E_{miss} range outside of the signal window.

3   Results

The SDME value for the entire kinematic region: $1.0 \ (\text{GeV}/c)^2 < Q^2 < 10.0 \ (\text{GeV}/c)^2$ with $\langle Q^2 \rangle = 2.4 \ (\text{GeV}/c)^2$, $0.01 \ (\text{GeV}/c)^2 < p_T^2 < 0.5 \ (\text{GeV}/c)^2$ with $\langle p_T^2 \rangle = 0.18 \ (\text{GeV}/c)^2$, $5.0 \ \text{GeV}/c^2 < W < 17.0 \ \text{GeV}/c^2$ with $\langle W \rangle = 9.9 \ \text{GeV}/c^2$ are presented in Fig. 3. The SDMEs were divided into five classes corresponding to different helicity transitions. For SDMEs in class A, the dominant contributions are related to the squared amplitudes for the transitions from longitudinal virtual photons to longitudinal vector mesons and from transverse virtual photons to transverse vector mesons. In class B, the dominant terms correspond to the interference of two above mentioned transitions. The SDMEs in classes C, D, and E are proportional to the amplitudes $\gamma_T^* \to V_L$, $\gamma_L^* \to V_T$ and $\gamma_T^* \to V_{-T}$, respectively. Non-zero elements are observed in classes A, B and C, while elements of classes D and E fluctuate near zero. The non-zero values of elements in class C indicate contributions from single-spin-flip process $\gamma_T^* \to V_L$.
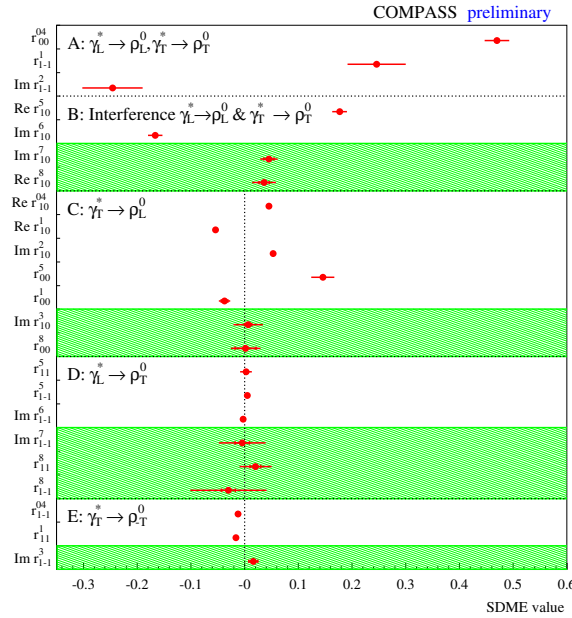
Figure 3: The 23 SDMEs for exclusive ρ^0 leptoproduction extracted for the entire COMPASS kinematic region with $\langle Q^2 \rangle = 2.4 \ (\text{GeV}c)^2$, $\langle p_T^2 \rangle = 0.18 \ (\text{GeV}c)^2$ and $\langle W \rangle = 9.9 \ (\text{GeV}c)^2$. The inter error bars represent statistical uncertainties and the outer ones statistical and systematic added in quadrature. The unpolarised (polarised) SDME are displayed as unshaded (shaded) areas.

The dependences of SDME on the kinematic variables Q^2, p_T^2 and W were also extracted. In Fig. 4 the dependences of SDMEs on Q^2 are presented. Similarly, as in the case for entire region the SDMEs were divided into classes. The elements from classes A and C are sensitive to Q^2 like r_{00}^{04} from class A and element r_{00}^5 from class C. In the case of r_{00}^{04} it is related to an increase of σ_L with Q^2. The dependences of SDMEs on W are rather flat (not shown).

The contributions of the spin-flip-transitions are described by the observables $\tau_{ij} = \frac{|T_{ij}|}{\sqrt{\mathcal{N}}}$, as combinations of SDMEs [11], where T_{01}, T_{10} and T_{1-1} are the amplitudes of the transitions $\gamma_T^* \to \rho_L^0$, $\gamma_L^* \to \rho_T^0$, $\gamma_T^* \to \rho_{-T}^0$, respectively, and $\mathcal{N}$ is a normalisation constant [11]. In Fig. 5 the dependence of the observables τ_{01}, τ_{10} and τ_{1-1} on Q^2, p_T^2 and W are presented. The observables values significantly different from zero for τ_{01} and much smaller ones for τ_{10}

and τ_{1-1} is consistent with different degrees of SCHC violation seen from SDMEs in classes C, D and E, respectively. The observables u_1, u_2 and u_3 are sensitive to amplitudes for UPE transitions. In particular, the UPE fractional contribution to the cross section is approximately given by $u_1/2$. The kinematic dependences of u_1, u_2 and u_3 are shown in Fig, 5 (right). We do not observe any significant UPE contribution in contrast to an large contribution fo exclusive omega muoproduction [12].
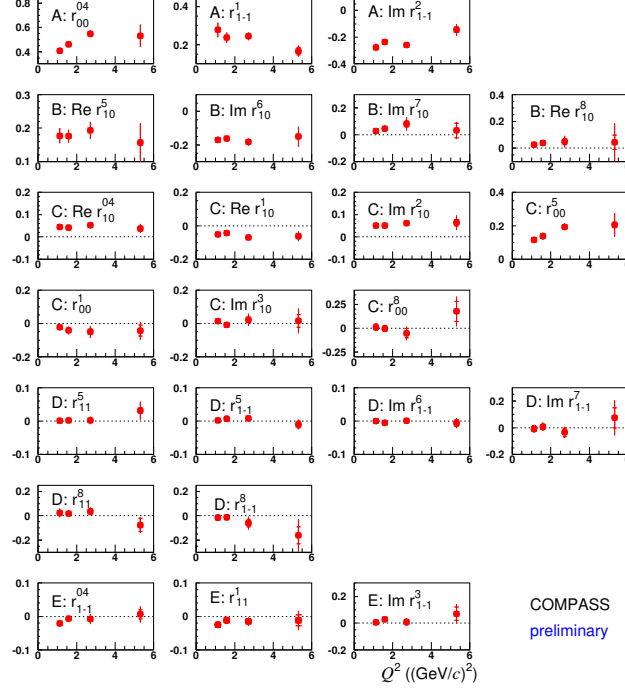
Figure 4: The dependences of SDMEs on Q^2. The SDMEs were divided into five classes the same as in Fig. 3.
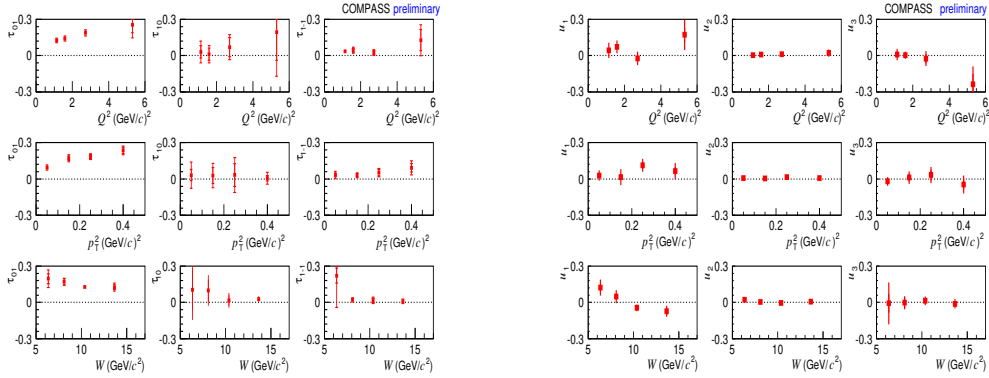
Figure 5: The dependences of τ_{01}, τ_{10} and τ_{1-1} (u_1, u_2 and u_3) on Q^2, p_T^2 and W in the left panel (right panel).

4   Conclusion

Spin Density Matrix Elements for exclusive leptoproduction of ρ^0 vector mesons were determined for the COMPASS kinematic region. The non-zero values of elements in class C indicate SCHC violation for transitions $\gamma_T^* \to \rho_L^0$. Clear Q^2 dependences of SDMEs for classes A, and element r_{00}^5 for class C are observed. No significant W dependence is observed. NPE processes are found to have dominant contributions.

Acknowledgements

This work is supported by the NCN Grant 2017/26M/ST2/00498 (Poland).

References

[1] J. C. Collins et al., *Phys. Rev. D* **56**, (2982) 1997, doi:10.1103/PhysRevD.56.2982.

[2] S. V. Goloskokov and P. Kroll, *Eur. Phys. J. C* **42**, (281) 2005, doi:10.1140/epjc/s2005-02298-5.

[3] S. V. Goloskokov and P. Kroll, *Eur. Phys. J. C* **50**, (829) 2007, doi:10.1140/epjc/s10052-007-0228-4.

[4] S. V. Goloskokov and P. Kroll, *Eur. Phys. J. C* **53**, (367) 2008, doi:10.1140/epjc/s10052-007-0466-5 .

[5] S. V. Goloskokov and P. Kroll, *Eur. Phys. J. C* **C59**, (809) 2008, doi:10.1140/epjc/s10052-008-0833-x.

[6] S. V. Goloskokov and P. Kroll, *Eur. Phys. J. C* **C74**, (2725) 2014, doi:10.1140/epjc/s10052-014-2725-6.

[7] K. Schilling and G. Wolf, *Nucl. Phys. C* **61** (361) 1973, doi:10.1016/0550-3213(73)90371-4 .

[8] A. Sandacz and P. Sznajder, "HEPGEN generator for hard exclusive leptoproduction", (2012), arXiv:1207.0333.

[9] P. Soeding, *Phys. Lett. B* **19**, (702) 1966.

[10] G. Ingelman et al. arXiv:hep-ph/9605286, doi:10.1016/S0010-4655(96)00157-9.

[11] A. Airapetian et al. (HERMES Collaboration), *Eur. Phys. J. C* **62** (659) 2009, doi:10.1140/epjc/s10052-009-1082-3 .

[12] G.D. Alexeev et al. (COMPASS Collaboration), *Eur. Phys. J. C* **81**, (126) 2021, doi:10.1140/epjc/s10052-020-08740-y.